Kinetics of structure formation in electrorheological suspensions

D. J. Klingenberg
Department of Chemical Engineering, University of Wisconsin, Madison, Wisconsin 53706

C. F. Zukoski
Department of Chemical Engineering, University of Illinois, Urbana, Illinois 61801

J. C. Hill[a)]
General Motors Research Laboratories, Warren, Michigan 48090-9055

(Received 13 November 1992; accepted for publication 22 December 1992)

Kinetics of structure formation in electrorheological (ER) suspensions are characterized by the time required to form percolating fibers following application of an external electric field. Experimental results are compared with predictions from simulations using an electrostatic polarization model for ER suspensions. Results from the two approaches agree, with large response times at small concentrations, decreasing to 10 ms at large concentrations and field strengths of 2 kV/mm.

I. INTRODUCTION

Electronic control of stress transfer with electrorheological (ER) suspensions is experiencing renewed interest. Devices currently being developed, including engine mounts and shock absorbers, require large field-induced viscosities as well as rapid responses, with times scales on the order of milliseconds. While a large body of research has been reported on the steady-state behavior of ER suspensions, little work has been reported on time-dependent aspects and the controlling mechanisms.

Previous studies have shown that the rheological response is intimately related to the field-induced fibrous structure, as originally postulated by Winslow.[1] The relation between rheology and suspension structure is similar to percolation on a random resistor network. Shear stress is transferred between the bounding surfaces by particulate strands that span the gap; prior to fiber formation, stress transfer at small shear rates is negligible. It follows that the kinetics of structure formation should be directly related to the kinetics of the rheological response. In particular, we expect the rheological response to evolve on a time scale similar to that of the structural response.

In this article, we compare experimental measurements of the kinetics of structure formation with predictions from dynamic simulation employing an electrostatic polarization model for ER suspension behavior. Formation kinetics are characterized by the time required to form percolating clusters in finite, two-dimensional, static systems.[2] Other methods are possible, including transient electrical (conductivity or dielectric constant), light scattering, and rheological measurements. We have chosen the present method for two reasons. First, observing the appearance of percolating clusters is straightforward in both experiments and simulations, with little or no data processing prior to comparison. Second, this method directly probes the fibrous structure which is intimately related to the rheological response.

In the following section, the simulation method and results are presented, followed by a description of the experimental technique and results in Sec. III. Comparison of the two approaches is discussed in Sec. IV. Predicted response times are found to agree well with experimental values, with rapid responses on the order of ten milliseconds at large particle concentrations and at an electric-field strength of 2 kV/mm.

II. SIMULATIONS

The kinetics of structure formation were investigated using the simulation method described in Refs. 3 and 4. ER suspensions are modeled as monodisperse suspensions of non-Brownian, hard, dielectric spheres immersed in a neutrally buoyant, nonconducting continuous phase. To facilitate comparison with experiments discussed in Sec. III, sphere positions are constrained to a monolayer perpendicular to the electrode surfaces. The spheres are subjected to electrostatic polarization forces induced by the applied electric field, and to hydrodynamic resistance due to their motion relative to the continuous phase. (See Refs. 3 and 4 for more detailed discussions of this model.)

The electrostatic forces are approximated by dipole interactions; each sphere polarizes under the applied field, appearing to a first approximation as a dipole aligned with the applied electric field $\mathbf{E}_0 = E_0\hat{\mathbf{z}}$. The force on a sphere of diameter σ at the origin due to another equal-sized sphere at (r,θ) is given by

$$\mathbf{F}_{el}(r,\theta) = F_0(\sigma/r)^4\,[(3\cos^2\theta - 1)\hat{\mathbf{e}}_r + \sin 2\theta\hat{\mathbf{e}}_\theta], \qquad (1)$$

where $F_0 = \frac{3}{16}\pi\epsilon_0\epsilon_c\sigma^2\beta^2E_0^2$ is the magnitude of the interaction (SI units). $\epsilon_0 = 8.8542\times10^{-12}$ F/m is the permittivity of free space, ϵ_c is the dielectric constant of the continuous phase, and $\beta = (\epsilon_p - \epsilon_c)/(\epsilon_p + 2\epsilon_c)$ characterizes the relative polarizability of the spheres of dielectric constant ϵ_p. $\hat{\mathbf{e}}_r$ and $\hat{\mathbf{e}}_\theta$ are unit vectors in the r and θ directions, respectively, where θ is the angle between the line of centers and the applied electric field. The total electrostatic force on each sphere is taken as the pairwise summation of interactions with all other spheres; the interaction with each elec-

[a)]Current address: 33 Devonshire Rd, Pleasant Ridge, MI 48069-1209.

 0021-8979/93/094644-05$06.00

trode is taken as the pairwise summation of the interactions with all particle images. This calculation ignores multipole and multibody contributions.

The hydrodynamic force on each sphere is treated as Stokes's drag,

$$\mathbf{F}_{\text{hyd}} = -3\pi\eta_c\sigma\frac{d\mathbf{r}}{dt}. \tag{2}$$

This approximation ignores all hydrodynamic interactions between spheres and between each sphere and the electrodes, as well as interactions between each sphere and the glass slide (Sec. III). The latter is difficult to describe because the distance between each sphere and the glass slide is unknown and likely varies from one sphere to another.

In addition to electrostatic and hydrodynamic forces, a hard-sphere repulsion is represented by the short-range function

$$\mathbf{F}_{\text{hs}} = F_0 \exp\left(-\frac{r/\sigma - 1}{0.01}\right)(-\hat{\mathbf{e}}_r), \tag{3}$$

with a similar form representing the hard-sphere/hard-wall interaction. Finally, based on experimental observation, spheres within a small distance from the electrode surface (0.05σ) are constrained in the direction parallel to the surface, and are only allowed to move perpendicular to the electrode.

Despite the approximations made in describing particle dynamics, this model for ER suspensions has successfully reproduced fibrous structures observed in ER suspensions,[3] as well as the qualitative behavior of the steady-state rheological response at small shear rates. However, multipole contributions to the electrostatic interaction are required to obtain the correct magnitude of the shear stress at small shear rates due to the importance of short-range interactions between spheres.[4] This is discussed further below.

From the force expressions arise natural length, force, and time scales: $l_s=\sigma$, $F_s=F_0$, and

$$t_s = 3\pi\eta_c\sigma^2/F_0 = 16\eta_c/\epsilon_0\epsilon_f\beta^2E_0^2.$$

Simulations produce dimensionless times and forces that are later converted to dimensional values given values for the system parameters. As discussed in Ref. 3, this model predicts that the suspension structure is independent of electric-field strength at long times—the magnitude of the field strength simply determines the time scale t_s. Hence, this model for ER suspension behavior implies that any measure of time characterizing the kinetics of structure formation will scale as $1/E_0^2$.

Simulations are started by randomly placing N spheres in a two-dimensional cell, with periodic boundaries in the direction parallel to the electrodes. To mimic the experimental conditions described in Sec. III, the electrode separation was set to $L_z=580$ μm, and the cell width to $L_x=970$ μm, with the sphere diameter $\sigma=47$ μm. Concentration is characterized by the area fraction $\phi=N\pi\sigma^2/4L_xL_z$. Sphere trajectories are determined by numerical integration of the equation of motion of each sphere, evaluating forces within a cutoff radius of five

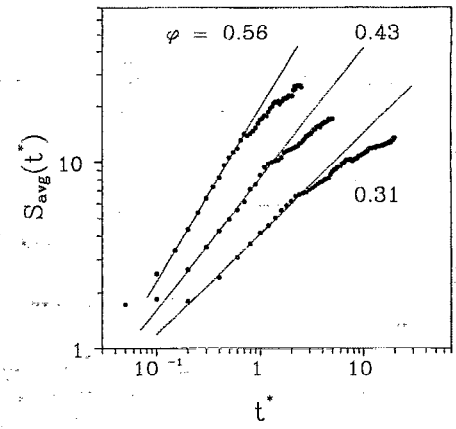

FIG. 1. Mean cluster size as a function of dimensionless time for several concentrations. ϕ is the area fraction of spheres in a two-dimensional monolayer.

sphere diameters. Integration was continued until particle motion ceased. For each concentration reported, 20 runs were performed with different initial configurations in order to obtain averages.

Following Ref. 5, formation kinetics were first probed by following the mean cluster size S_{avg} as a function of time,

$$S_{\text{avg}}(t^*) = \frac{\Sigma_s N_s(t^*)s^2}{\Sigma_s N_s(t^*)s} = \frac{1}{N}\sum_{k=1}^{N_c} m_k^2(t^*), \tag{4}$$

where $t^*=t/t_s$ is the dimensionless time, $N_s(t^*)$ is the number of clusters containing s spheres, N_c is the total number of clusters, and m_k is the number of spheres in the kth cluster. Cluster statistics were evaluated using the connectivity matrix method,[3,6] where sphere pairs with separations $r<\sigma+\delta$ are considered directly connected. Calculations were performed with $\delta/\sigma=0.01$, 0.02, 0.03, and 0.04, followed by extrapolation to $\delta=0$.

The mean cluster size, averaged over all simulation runs, is plotted as a function of time for three different concentrations in Fig. 1. At small times, the mean cluster size is a power-law function of time, $S_{\text{avg}}(t^*) \propto t^{*n(\phi)}$, and the exponent $n(\phi)$ increases with concentration [$n(\phi=0.12)=0.32$, $n(\phi=0.56)=0.93$]. At a certain time, each curve abruptly deviates from this power-law behavior, with $S_{\text{avg}}(t^*)$ increasing more slowly with time. This change is due to clusters coming into contact with the electrodes, which prohibits motion parallel to the surfaces, thereby inhibiting aggregation. The time at which the break occurs corresponds to the appearance of a percolating cluster in the periodic cell, as well as to the maximum in the adjusted mean cluster size distribution (the mean cluster size [Eq. (4)] not counting percolating clusters).

See and Doi[5] simulated structure formation in ER suspensions in a similar manner, but obtained significantly different results. They found that $S_{\text{avg}}(t^*)$ followed power-law behavior at large times, with the exponent n independent of concentration; this behavior continued without the abrupt change discussed above. The different results are likely due to two important differences in the simulated

systems. See and Doi used a longer-range function to represent the hard-sphere repulsion; using the present notation, $\mathbf{F}_{hs}^{See}/F_0=2(\sigma/r)^{13}(-\mathbf{e}_r)$. This form has been shown to produce only single-sphere-width chains due to its longer range masking weak relative potential-energy minima at triangular lattice positions alongside the chains.[3] Hence, this form for the short-range repulsive interaction is only expected to be valid for very dilute suspensions where only single-sphere-width chains are indeed observed.

Another significant difference is that See and Doi simulated a two-dimensional system that is periodic in both directions, instead of incorporating electrodes, which influences particle dynamics in two ways. Spheres near an electrode interact with their own images as well as the images of neighboring spheres. In contrast, in a completely periodic system, spheres near a periodic boundary interact with images of more distant spheres. It is uncertain to what extent this correlation effect will influence structure evolution. A more significant effect of the electrodes in the present model is that spheres "touching" an electrode surface are prohibited from moving parallel to the electrode. This feature, based on experimental observation, inhibits aggregation and produces the abrupt change in $S_{avg}(t^*)$ discussed above. We note that we have performed simulations using the longer-range repulsive force used by See and Doi, and again found power-law behavior for $S_{avg}(t^*)$ at small times, with an exponent that depends on concentration, followed by the abrupt change arising from electrode interactions.

As mentioned previously, we expect the appearance of percolating clusters to represent a significant event in the evolution of the rheological response, especially at small shear rates.[3] Hence, we choose to characterize structure formation kinetics in terms of this percolation time, using Eq. (3) to represent hard-sphere repulsion. In the following section, results of experimental measurements of the percolation time are presented.

The percolation time, defined as the time required to form the first percolating cluster, was calculated for each run and averaged as follows:

$$t_{p,\mathrm{avg}}^{*-1}=\frac{1}{N_{\mathrm{runs}}}\sum_{i=1}^{N_{\mathrm{runs}}} t_{p,i}^{*-1}. \tag{5}$$

We choose to average rates instead of times because some runs did not produce percolating clusters (giving infinite percolation times) and the corresponding distributions were much less skewed.

Results from simulations performed at concentrations ranging from $\phi=0.12$–0.70 are plotted in Fig. 2 (along with experimental data discussed below). The solid circles represent averages over all simulation runs at the respective concentrations. Three features of the results are apparent: the sensitive dependence of the response time on particle concentration, the considerable scatter in the data, and the saturation at large concentrations. The response time decreases by several orders of magnitude over the range of concentrations shown, with dimensional times (see below) at large concentrations on the order of 10 ms for a field strength of 2 kV/mm. The error bars in Fig. 2

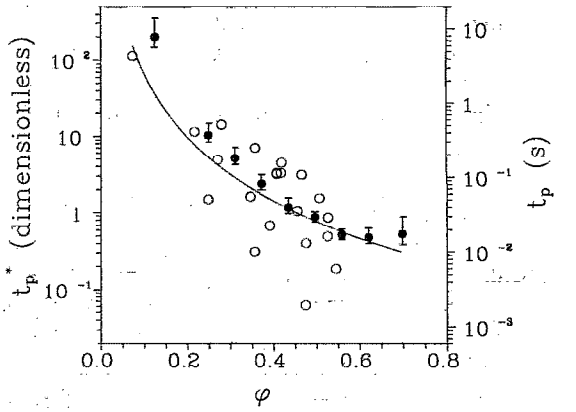

FIG. 2. Percolation time as a function of particle concentration. Solid circles represent all simulation results averaged at each concentration, open circles represent experimental data, and the solid line is the least-squares fit of the experimental data to Eq. (6). ϕ is the area fraction of spheres in a two-dimensional monolayer.

represent the significant variation in percolation times from one simulation to another, demonstrating the sensitivity of structure evolution to the initial configuration. Saturation of the response time at large concentration is discussed in Sec. IV.

The following parameter values were used to convert dimensionless quantities obtained from simulations to values comparable with the experiments: $E_0=2.0\times10^6$ V/m, $\eta_c=0.048$ Pa s, $\epsilon_c=2.7$, $\beta=0.5$. The resulting time scale is $t_s=0.0321$ s. The value of β is based on the measured dielectric constant for silica spheres hydrated by exposure to ambient room humidity.[4] Although simulated response times are proportional to $1/\beta^2$, the major conclusions of this work are insensitive to the precise value of β.

III. EXPERIMENT

The experimental setup and procedure have been described previously.[7] Here we review the details pertinent to the current discussion.

The suspensions consisted of hydrated glass spheres (diameter $\sigma=47\pm5$ μm) in a silicone transformer oil continuous phase (Dow Corning 561, dielectric constant $\epsilon_c=2.71$, density $\rho_c=960$ kg/m^3, viscosity $\eta_c=0.048$ Pa s). Suspension dynamics were observed in a horizontal cell consisting of electrodes glued to a glass slide, separated by 580 μm. The field of view in the video display parallel to the electrodes was 970 μm. These dimensions are identical to those used in the computer simulations. The spheres (denser than the oil) settled on the glass slide, producing a two-dimensional monolayer.

Structure formation was observed with a Spin Physics high-speed motion analysis system operating at 1000 frames/s, using a dc electric field of 2 kV/mm applied through a mercury-wetted relay, producing a rise time of ≈20 μs (results under alternating electric fields are similar to those reported here).[7] The recorded response time was defined as the time required to form the first percolating cluster after application of the electric field. The area frac-

tion ϕ was determined by counting the total number particles in a video frame, multiplying by the projected area per particle, and dividing by the total visible area between the electrodes. Uncertainties in the response times and concentrations are $\pm 4\times 10^{-3}$ s and $\pm 15\%$, respectively.

Response times for 21 experiments are plotted as a function of area fraction in Fig. 2, along with the simulation results. The prevalent features of the simulation results are reproduced by the experiments—the sensitive dependence of the response time on particle concentration and the considerable scatter in the data. Times are on the order of milliseconds at large concentrations, increasing to seconds at small concentrations. The apparent divergence at small concentrations (response time approaching infinity as $\phi \to 0$) is further demonstrated by several experiments in which percolating clusters did not form (not included in Fig. 1). The scatter in the data, also observed in Ref. 7, is not attributed to uncertainty, implying that the response time is sensitive to the initial configuration of spheres. As discussed above, this behavior is also observed in the simulation of structure formation.

IV. DISCUSSION

For $\phi \lesssim 0.55$, the simulation results mimic the behavior exhibited by the experiments—a rapid response at large concentrations and an apparent divergence at small concentrations (Fig. 2). At large concentrations, experiments and simulations yield a response time (at 2 kV/mm) on the order of 10 ms. This sensitive concentration dependence has been observed previously,[3,7] but the agreement here between experiments and simulations, with no adjustable parameters, demonstrates the validity of the electrostatic polarization mechanism in predicting not only the observed structures but also the kinetics of structure formation.

The extent of quantitative agreement is somewhat surprising given the approximations in the simulation model (e.g., dipole interactions, Stokes' law, periodic boundary conditions, etc.), as well as nonidealities in the experimental system (including deviations from monolayer structure, friction between spheres and the glass slide, nonuniform electric-field strength across the gap, and polydispersity in particle diameter). We have previously found that the yield stress predicted from this model is significantly smaller than experimental values unless higher-order electric multipole contributions to the electrostatic interaction, which are significant at small sphere separations, are incorporated.[4] Hence, we may attribute the success in predicting the suspension structure and response times to structure formation being dominated by motions at large separations where the dipole approximation is valid. Another factor facilitating agreement is that increased attraction between spheres due to higher-order electric multipoles is partly compensated by hydrodynamic lubrication, both of which are neglected in the present model.

The behavior shown in Fig. 2 can be quantified by fitting the response times to a power-law function of the particle concentration,

TABLE I. Coefficients for the power-law fit of the percolation time as a function of particle concentration [Eq. (6)]: (a) using all simulation results averaged at each concentration; (b) using only results for percolating clusters. $\sigma_{\ln a}$ and σ_b are the standard errors in $\sigma_{\ln a}$ and b, respectively.

	a	b	$\sigma_{\ln a}$	σ_b
Experiments	0.12	−2.8	0.63	0.6
Simulations (a)	0.050	−3.9	0.11	0.1
Simulations (b)	0.096	−3.2	0.19	0.2

$$t_p^* = t_p/t_s = a\phi^b, \tag{6}$$

where a and b are independent of ϕ. Values of the parameters a and b obtained from a least-squares fit are presented in Table I for the experimental data, the simulation results averaged at each concentration, and again using the simulation results averaged over only those runs producing percolating clusters. The simulations excluding the nonpercolating data give results quite similar to the experiments, while including the nonpercolating realizations gives a significantly larger exponent (in magnitude).

The gross features of $t_p(\phi)$ can be explained by considering the average pair separation prior to application of the electric field. Large times at small ϕ result from the large distances particles must travel to aggregate. Response times decrease as the concentration increases and average particle separation decreases. A precise description at small and large concentrations is difficult, however, requiring detailed consideration of particle motions and suspension structure.

At vanishing concentrations, infinite response times are expected when there are not enough particles present to span the electrode gap. This threshold must depend on the particular configuration (for finite systems), because infinite times were occasionally observed at concentrations known to produce percolating clusters. The location of this lower threshold is also expected to depend on the particular definition of response time (i.e., averaging procedure) and will be a function of the system size.

Simulated response times saturate for $\phi \gtrsim 0.6$. We note that crystalline domains (triangular lattice) were observed in the initial configurations in this region. Their presence may be due to the proximity to the hard-disk phase transition, which is shifted to smaller concentrations due to the planar electrodes.[8] (The location of this phase transition could be determined, but has not been for the present system.) One possible explanation for the saturation of percolation times is that crystallites are metastable and hence less inclined to rearrange under the influence of the electric field; nearest-neighbor spheres within crystallites reside in local-energy minima, relying on distant spheres and weaker forces to determine their motion.

In addition to the proximity to the phase transition, interpretation in this concentration range is further complicated by the uncertain relevance of the percolation threshold for $E=0$. That is, a cluster percolating under no applied field may rearrange into a nonpercolating cluster after the polarization interactions are introduced. Unfortu-

nately, it was not possible to examine this regime experimentally, because the system deviated significantly from a monolayer.

The details at very small and large concentrations are interesting, but are probably of little importance for practical ER applications—large concentrations possess excessive zero-field viscosities while small concentrations respond slowly and exhibit only modest ER activity. Hence, over practical ranges in concentrations, the concentration dependence of the formation kinetics are well characterized by the power-law form [Eq. (6)].

We close with a brief discussion of some related, preliminary results. Experiments on hollow silica spheres in corn oil display similar behavior to the results presented here, under both ac and dc electric fields, and in agreement with the simulation model, response times are found to vary as $1/E_0^2$.[9] Preliminary simulations in three dimensions also show similar behavior.[10] Finally, we note that the power-law exponent b in Eq. (6) is a weak function of the ratio of the electrode gap width to sphere diameter; simulations show that the response time decreases more rapidly as concentration increases for larger electrode gaps.

V. CONCLUSIONS

The kinetics of structure formation in ER suspensions has been found to depend sensitively on particle concentration, with response times on the order of 10 ms at large concentrations and field strengths of 2 kV/mm. The agreement between experimental and simulated kinetics, with no adjustable parameters, suggests that the electrostatic polarization mechanism, treated here in the point-dipole limit, provides an adequate description of particle dynamics and demonstrates that structure formation is dominated by interactions between distant particles where the dipole approximation is valid. In contrast, it has been shown that the shear stress in ER suspensions is quite sensitive to higher-order moments of the charge distribution and short-range forces.[4] This suggests that the kinetics of the rheological response, while related to the kinetics of structure formation, may exhibit different behavior, and therefore requires direct investigation.

[1] W. M. Winslow, J. Appl. Phys. **20**, 1137 (1949).
[2] See T. C. Halsey and W. Toor, Phys. Rev. Lett. **65**, 2820 (1990) for a discussion of structure evolution kinetics following formation of the initial, columnar structure.
[3] D. J. Klingenberg, F. van Swol, and C. F. Zukoski, J. Chem. Phys. **91**, 7888 (1989).
[4] D. J. Klingenberg, F. van Swol, and C. F. Zukoski, J. Chem. Phys. **94**, 6160 (1991); **94**, 6170 (1991).
[5] H. See and M. Doi, J. Phys. Soc. Jpn. **60**, 2778 (1991).
[6] E. M. Sevick, P. A. Monson, and J. M. Ottino, J. Chem. Phys. **88**, 1198 (1988).
[7] J. C. Hill and T. H. Van Steenkiste, J. Appl. Phys. **70**, 1207 (1991).
[8] F. B. van Swol (personal communication).
[9] P. J. Malone, D. J. Klingenberg, and C. F. Zukoski (unpublished).
[10] D. J. Klingenberg and C. F. Zukoski (unpublished).